Adsorption of atomic nitrogen and oxygen on $ZnO(2\bar{1}\bar{1}0)$ surface: a density functional theory study

2009 J. Phys.: Condens. Matter 21 144208

(http://iopscience.iop.org/0953-8984/21/14/144208)

IOP PUBLISHING JOURNAL OF PHYSICS: CONDENSED MATTER

J. Phys.: Condens. Matter **21** (2009) 144208 (10pp) doi:10.1088/0953-8984/21/14/144208

Adsorption of atomic nitrogen and oxygen on ZnO($2\bar{1}\bar{1}0$) surface: a density functional theory study

M Breedon[1,2], M J S Spencer[1] and I Yarovsky[1]

[1] Applied Physics, School of Applied Sciences, RMIT University, GPO Box 2476V, Vic 3001, Australia

[2] School of Electrical and Computer Engineering, RMIT University, GPO Box 2476V, Vic 3001, Australia

E-mail: irene.yarovsky@rmit.edu.au

Received 28 August 2008, in final form 25 September 2008

Published 18 March 2009

Online at stacks.iop.org/JPhysCM/21/144208

Abstract

The adsorption of atomic nitrogen and oxygen on the ($2\bar{1}\bar{1}0$) crystal face of zinc oxide (ZnO) was studied. Binding energies, workfunction changes, vibrational frequencies, charge density differences and electron localization functions were calculated. It was elucidated that atomic oxygen binds more strongly than nitrogen, with the most stable O/ZnO($2\bar{1}\bar{1}0$) structure exhibiting a binding energy of −2.47 eV, indicating chemisorption onto the surface. Surface reconstructions were observed for the most stable minima of both atomic species. Positive workfunction changes were calculated for both adsorbed oxygen and nitrogen if the adsorbate interacted with zinc atoms. Negative workfunction changes were calculated when the adsorbate interacted with both surface oxygen and zinc atoms. Interactions between the adsorbate and the surface zinc atoms resulted in ionic-type bonding, whereas interactions with oxygen atoms were more likely to result in the formation of covalent-type bonding. The positive workfunction changes correlate with an experimentally observed increase in resistance of ZnO conductometric sensor devices.

(Some figures in this article are in colour only in the electronic version)

1. Introduction

ZnO has been popularized as a versatile material existing in numerous nanodimensional forms, with many potential applications encompassing: piezoelectric energy generation [1], solar cells [2], catalysis [3], gas sensors [4], as a photonic material [5] and useful in electronics as a wide band gap semiconductor [6]. A large number of ZnO nanomaterials have been synthesized, which include but are not limited to: nanocages, nanocombs, nanorings, nanosprings, nanobows, nanorods, nanocastles and nanodisks [7]. All hexagonal ZnO nanomaterials preferentially expose the {$2\bar{1}\bar{1}0$} crystal face with other low energy crystal faces also being present. Nanostructures that are dominated by large ($2\bar{1}\bar{1}0$) facets include: nanobelts [8], nanosprings, nanohelices and nanobows [9].

The large surface area of nanostructured ZnO materials (such as arrays) makes them ideal candidates for gas sensing technologies and have been employed in detecting a range of gases, including CO, H_2S, HCHO, CH_3CH_2OH, NO, NO_2, NH_3, H_2 [4, 10, 11] with successful applications in Schottky diode based sensing [12], conductometric [13], and surface acoustic wave [11] technologies.

Theoretical adsorption studies on clean ZnO surfaces tend to focus on the non-polar ($10\bar{1}0$) or (0001) polar surfaces of ZnO, or the effects that stoichiometric disruptions to their crystal lattice (typically in the form of vacancies) have on their surface chemistry (see for example [14–21]). Likewise there have been few studies that have examined adsorption on the ($2\bar{1}\bar{1}0$) surface. Most recently Wang *et al* [22] has presented a study on the effects of atomic hydrogen adsorption on the electronic properties of a ZnO nanowire with a ($2\bar{1}\bar{1}0$) surface, indicating that the electronic character of the ($2\bar{1}\bar{1}0$) surface may become more metallic upon hydrogen adsorption.

To the best of our knowledge, density functional theory adsorption studies on the ($11\bar{2}0$) surface are limited to H_2 [23]

and H_2O [15]. Cooke *et al* [15] investigated atomic hydrogen, hydroxyl and water adsorbed onto the ZnO(11$\bar{2}$0) surface, generating a phase diagram outlining the likely surface species present at different partial pressures of oxygen and hydrogen and identifying the most stable (11$\bar{2}$0) surfaces were those that were either stoichiometric (i.e. clean) or covered with a monolayer of water. Nyberg *et al* [23] investigated the adsorption of molecular hydrogen on both the (10$\bar{1}$0) and (11$\bar{2}$0) ZnO surfaces and found that molecular hydrogen did not dissociatively adsorb.

Adsorption of molecular oxygen has been studied on the stoichiometric and non-stoichiometric ZnO(10$\bar{1}$0) surface by Yan *et al* [24]. It was observed that molecular oxygen can dissociatively adsorb onto a stoichiometrically deficient (1010) surface, and that bridging oxygen atoms can migrate to neighbouring oxygen defects in the surface model to restore stoichiometry. There do not appear to be any studies of atomic nitrogen or oxygen on ZnO(2$\bar{1}\bar{1}$0).

Atomic species such as nitrogen and oxygen are of importance as they may be involved in the dissociative adsorption of larger molecular species such as CO, O_2, N_2 and NO_x which, are derived from both natural process and anthropogenic sources [25, 26]. Additionally, atomic species are also of interest to upper atmosphere scientists and aerospace engineers, as low earth orbit presents its own unique set of environmental conditions. Osborne *et al* [27] reported the use of sputtered ZnO thin films for the detection of atomic oxygen in low earth orbit (180–650 km). The qualification and subsequent monitoring of atomic oxygen is of vital importance to space-borne vehicles, which suffer from the degradative effects of such reactive atomic oxygen fluxes, limiting their operational lifespan. Understanding the interaction between atomic species and different surfaces of ZnO may assist in the successful implementation of ZnO based technologies for low earth orbit sensing.

In this paper the adsorption of nitrogen and oxygen on the ZnO(2$\bar{1}\bar{1}$0) crystal face is examined using DFT calculations. The adsorption geometries, binding energy, workfunction changes, charge density, electron localization function have been determined and compared for the two atomic adsorbates.

2. Method

2.1. Computational methodology

All calculations were performed using the Vienna *Ab initio* Simulation Package (VASP) [28–30], which performs fully self-consistent density functional theory (DFT) calculations to solve the Kohn–Sham equations [31]. The generalized gradient approximation utilizing the functional of Perdew and Wang (PW91) [32] was employed. Core electrons were replaced with ultra-soft pseudopotentials as implemented in the VASP package [33]. The electronic wavefunctions were expanded as a linear combination of plane waves, and truncated to include only plane waves with kinetic energies less than 400 eV. K-space sampling was performed using the Monkhorst and Pack scheme [34] with a mesh of 5 × 5 × 1. The isolated oxygen and nitrogen atoms were modelled in a 10 Å × 10 Å × 10 Å supercell.

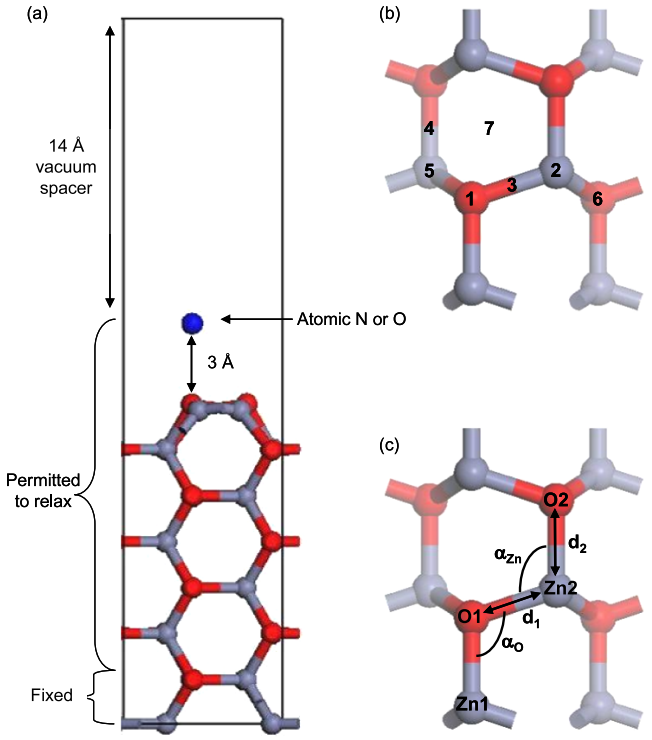

Figure 1. (a) ZnO(2$\bar{1}\bar{1}$0) surface model (oxygen atoms denoted in red, zinc atoms in grey); (b) top view of surface showing high symmetry surface adsorption sites: 1—atop O; 2—atop Zn; 3—upper Zn–O bridge; 4—lower Zn–O bridge; 5—lower atop zinc; 6—lower atop O; 7—hollow; (c) parameters measuring surface geometry.

2.2. Surface models

ZnO surfaces were modelled using the supercell approach, where periodic boundary conditions are applied to a central supercell, so that it is repeated periodically throughout three dimensional space. The non-polar (2$\bar{1}\bar{1}$0) surface was cleaved from the bulk wurtzite structure of ZnO with optimized lattice constants of $a = b = 3.268$ Å, $c = 5.233$ Å [35]. A vacuum spacing of 14 Å was introduced in the z-direction. Modelling of adsorption was achieved by initially placing an oxygen or nitrogen atom ∼3 Å above an 8 layer (32 atom) ZnO(2$\bar{1}\bar{1}$0) surface. The surface energy for this sized slab was previously determined to be converged to 0.01 J m^{-2} [35]. The seven top surface layers, as well as the adsorbate atom, were allowed to relax in the x-, y-, z-directions, while keeping the bottom surface layer fixed. The atomic positions were optimized until the total energy converged to 0.01 eV and the Hellmann–Feynman force on each atom that was relaxed was less than 10^{-4} eV. Seven unique adsorption sites were investigated, including: atop zinc and oxygen sites, lower Zn–O bridge, upper Zn–O bridge and hollow sites (figure 1(b)).

The binding energy (BE) calculations were performed as per

$$\mathrm{BE} = [E_{\mathrm{ads+surf}} - (E_{\mathrm{ads}} + E_{\mathrm{clean}})] \quad (1)$$

where $E_{\mathrm{ads+surf}}$ is the total energy of the relaxed O/ZnO(2$\bar{1}\bar{1}$0) or N/ZnO(2$\bar{1}\bar{1}$0) system; E_{ads} is the total energy of the free adsorbate; and E_{clean} is the total energy of the clean ZnO(2$\bar{1}\bar{1}$0) surface. Hence, a negative binding energy indicates favourable

Table 1. Calculated parameters for minimum energy structures of O on ZnO($2\bar{1}\bar{1}0$). (Note: binding energy, BE; workfunction change, $\Delta\Phi$; perpendicular distance between the top surface layer and adsorbate, $d^{\perp}$; distance between adsorbate and surface, d(ads-surf); symmetric vibrational frequency of the adsorbed species, V_{Sym}.)

Structure	BE (eV)	$\Delta\Phi$ (eV)	Bonded to	d(ads-surf) (Å)	$d^{\perp}$ (Å)	ν_{sym} (cm^{-1})
1_{O}	−2.47	−0.04	Zn, Zn, O	2.39, 1.95, 1.50	0.25	595
2_{O}	−1.55	0.03	Zn	1.96	0.54	362
3_{O}	−1.55	0.50	Zn, Zn	2.08, 1.95	1.18	397

Table 2. Calculated for minimum energy structures of N on ZnO($2\bar{1}\bar{1}0$). (Note: binding energy, BE; workfunction change, $\Delta\Phi$; perpendicular distance between the top surface layer and adsorbate, $d^{\perp}$; distance between adsorbate and surface, d(ads-surf); symmetric vibrational frequency of the adsorbed species, V_{Sym}.)

Structure	BE (eV)	$\Delta\Phi$ (eV)	Bonded to	d(ads-surf) (Å)	$d^{\perp}$ (Å)	ν_{sym} (cm^{-1})
1_{N}	−1.42	−1.13	Zn, Zn, O	2.15, 2.01, 1.39	0.19	759
2_{N}	−1.16	−1.27	Zn, O	2.12, 1.39	0.43	681
3_{N}	−0.12	0.07	Zn	2.07	1.68	297

adsorption, whereas a positive binding energy indicates an unstable system. To classify the type of stationary points determined by the geometry optimization, vibrational frequency calculations were performed by permitting directional freedom to the adsorbate in the x-, y-, z-directions, while fixing all of the surface atoms, and diagonalizing a finite difference construction of the Hessian matrix with displacements of 0.015 Å. Only minimum energy structures (i.e. those with only real vibrational frequencies) are reported here.

Workfunction (Φ) values were calculated using the following equation [36]

$$\Phi = E_{\mathrm{Vac}} - E_{\mathrm{F}} \tag{2}$$

where E_{Vac} is the electrostatic potential in the vacuum region of the supercell on the adsorbate side and E_{F} is the Fermi level energy. Similarly, workfunction changes ($\Delta\Phi$) were calculated with the following equation

$$\Delta\Phi = (\Phi - \Phi_{\mathrm{C}}) \tag{3}$$

where Φ_{C} is the workfunction of the clean ZnO($2\bar{1}\bar{1}0$) surface.

3. Results and discussion

3.1. Geometry and binding energies

The calculated binding energy values for the O/ZnO($2\bar{1}\bar{1}0$) and N/ZnO($2\bar{1}\bar{1}0$) systems are presented in tables 1 and 2, respectively. There were three local minimum energy structures found for each adsorbate. The most stable oxygen adsorbate (structure 1_{O}) had a binding energy of −2.47 eV, while the most stable nitrogen adsorbate (structure 1_{N}) had a binding energy of −1.42 eV, indicating that oxygen binds more strongly on the ZnO($2\bar{1}\bar{1}0$) surface. The other two oxygen local minima (structures 2_{O} and 3_{O}) have the same binding energy value of −1.55 eV. For the other nitrogen structures, the second most stable site (structure 2_{N}) has a binding energy of −1.16 eV, while the least stable structure (structure 3_{N}) has a much smaller binding energy of −0.12 eV. The magnitude of the binding energy of the most stable systems indicates that oxygen and nitrogen are chemisorbed on the surface. Conversely, the small binding energy of the least stable nitrogen structure indicates that the interaction is very weak, suggesting physisorption.

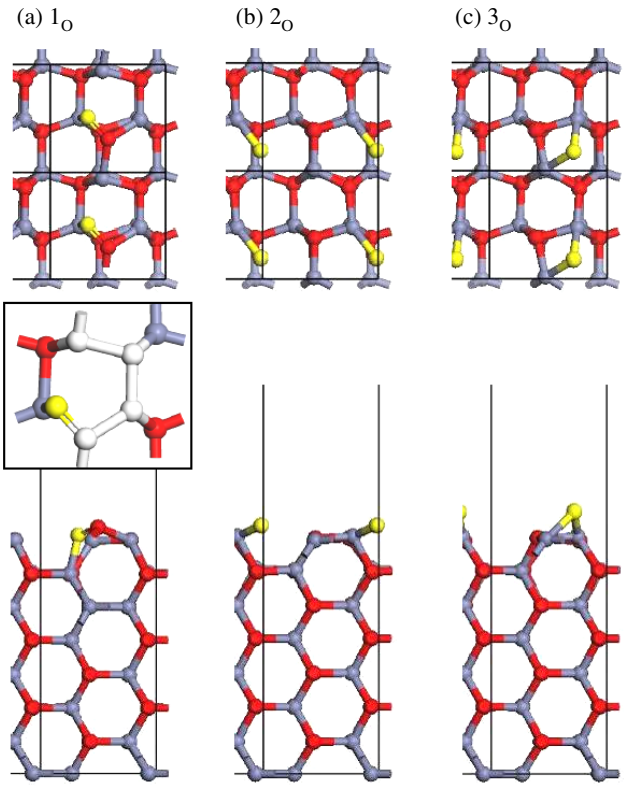

Figure 2. Optimized geometries of the three local minimum structures for O/ZnO($2\bar{1}\bar{1}0$), showing structures (a) 1_{O}, (b) 2_{O} and (c) 3_{O}. Inset of (a) shows enlarged view of adsorbate and top layer atoms. Surface oxygen atoms denoted in red, zinc atoms in grey, oxygen adsorbate atom in yellow (for clarity), other top layer atoms of structure 1_{O} inset in white.

The geometries of these six structures are presented in figures 2 and 3. The distances between the top surface layer and the adsorbate, (measured as the height of the adsorbate on the top surface plane) as well as the shortest adsorbate to

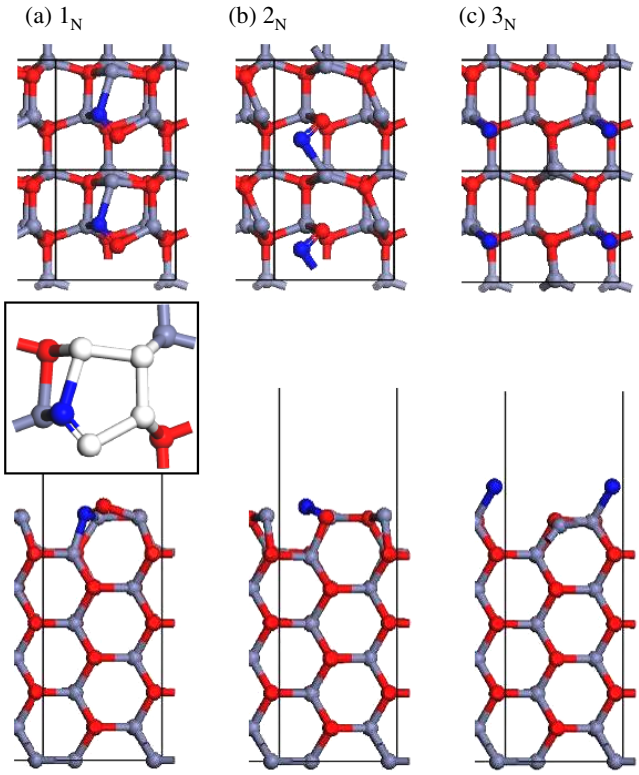

Figure 3. Optimized geometries of the three local minimum structures for N/ZnO($2\bar{1}\bar{1}0$), showing structures (a) 1_N, (b) 2_N and (c) 3_N. Inset of (a) shows enlarged view of adsorbate and top layer atoms. Surface oxygen atoms denoted in red, zinc atoms in grey, nitrogen adsorbate atom in blue, other top layer atoms of structure 1_N inset in white.

surface atom distance for the O/ZnO($2\bar{1}\bar{1}0$) and N/ZnO($2\bar{1}\bar{1}0$) systems are presented in tables 1 and 2, respectively.

It was found that both atomic species will preferentially adsorb on the surface in more highly coordinated sites, as seen in figures 2 and 3. The geometries of the most stable oxygen and nitrogen systems are very similar, with either adsorbate interacting with two neighbouring zinc atoms as well as one neighbouring oxygen surface atom. The geometry of the other minima are also very similar to each other, with one structure showing the adsorbate bonding to two surface atoms (structures 3_O and 2_N). It is noteworthy that oxygen bonds to two surface Zn atoms, whilst nitrogen bonds to one zinc and one oxygen atom. For the other minima, both oxygen and nitrogen only bond to one surface zinc atom (structures 2_O and 3_N).

The upper layer of the clean ZnO surface comprises two zinc atoms and two oxygen atoms arranged into a hexagonal pattern which can be seen in figure 1. For the most stable oxygen and nitrogen structures, the adsorbate atom was found to integrate itself into the upper layer of the terraced ($2\bar{1}\bar{1}0$) surface. Interestingly, when the nitrogen adsorbate incorporates itself into the top layer (figure 1(a)), it forms a distorted 5-membered ring with the top layer ZnO surface atoms (inset figure 3(a)). Atomic oxygen was also found to integrate itself in a similar manner (inset figure 2(a)).

In these integrated systems, the shortest distances are between the adsorbate atom and a surface oxygen atom, resulting in the formation of an O–O bond or an N–O bond, that are shorter than the clean Zn–O bond length of 1.96 Å in the relaxed surface. Here the O–O bond is 1.52 Å, which is 0.29 Å longer than the molecular bond length for O_2 of 1.23 Å. Similarly, the N–O bond was measured to be 1.39 Å, which is 0.22 Å longer than the molecular NO bond length of 1.17 Å. The increase in these distances compared to the free molecule is due to the fact that oxygen and nitrogen are also bonded to other surface atoms, reducing their interaction with the closest surface atom and lengthening the bond.

As can be seen in the top view of structure 3_O (figure 2(c)), the chemisorbed oxygen forms a bridging bond between two surface zinc atoms, positioning itself over the hollow site that is formed by the hexagonal terraced structure of wurtzite ZnO. Importantly, the O–Zn adsorbate–substrate bond length is identical to those found in the relaxed ZnO surface (1.96 Å). Additionally, the height of the adsorbate above the upper layer is 1.52 Å which is only slightly larger than the first interlayer distance of 1.42 Å, indicating that oxygen adsorbs so as to retain the surface geometry.

The shortest distance between the adsorbate and substrate atoms was observed in the integrated surface models, being as low as 1.39 Å for atomic nitrogen bonded to a surface oxygen atom (figure 3(a)). The distance between the top surface layer and the adsorbate was found to be less than 2 Å for all six minima. The shortest adsorbate-surface distance was 0.19 Å for the three-fold adsorption of atomic nitrogen (structure 1_N) reflecting the integration of the adsorbate into the top surface layer. While the largest distance measured for the adsorption of atomic nitrogen onto the atop zinc site was 1.68 Å (structure 3c), indicating physisorption.

3.2. ZnO($2\bar{1}\bar{1}0$) relaxation and reconstruction upon adsorption

The displacements of atoms in the top two layers of the surface after atomic adsorption are reported in table 3 (oxygen) and table 4 (nitrogen). Relaxation of the two zinc and two oxygen surface atoms (movement in the direction perpendicular to the surface plane, i.e. z-axis) is referenced against their original positions in the relaxed clean surface. Here, negative values represent a movement towards the bulk (contraction) and positive values indicate a displacement away from the surface (expansion). Reconstructions on the other hand, occur when the surface atoms move in the x- and y-directions of the surface.

The first interlayer spacing of the relaxed clean ZnO($2\bar{1}\bar{1}0$) surface is 1.52 Å, while the second to third layer separation is relatively larger measuring 1.68 Å. Buckling (an uneven movement of the atoms in the z-axis) was seen for all minimum energy structures, where the surface oxygen atom relaxed by a different amount to the surface zinc atom. This was most predominant in the first layer, with the largest displacement being 0.74 Å. The average displacement of either oxygen or zinc in this layer (regardless of whether the movement is a contraction or expansion of the layer) for any of the structures was 0.12 Å. Buckling also occurred in the second layer but to a lesser extent with displacements up to

Table 3. Atomic displacements (Å) upon adsorption of atomic oxygen on ZnO($2\bar{1}\bar{1}0$). (Note: α_{Zn} is the O–Zn–O angle; α_O is the Zn–O–Zn angle; d_1 and d_2 are the surface Zn–O bond distances, as shown in figure 1(c).)

	Reconstruction				Relaxation							
Structure	α_{Zn} (deg)	α_O (deg)	d_1 (Å)	d_2 (Å)	Layer 1				Layer 2			
Clean ZnO	119.6	105.4	1.90	1.88	Zn 1	Zn 2	O 1	O 2	Zn 1	Zn 2	O 1	O 2
1_O	120	117	1.95	1.89	0.08	0.10	0.74	0.12	0.03	−0.06	−0.06	−0.03
2_O	100	107	1.93	1.93	−0.07	0.14	0.05	0.05	0.09	0.01	−0.11	−0.03
3_O	107	92	2.03	1.90	0.14	−0.07	0.04	0.05	0.01	0.09	−0.04	−0.11

Table 4. Atomic displacements (Å) upon adsorption of atomic nitrogen on ZnO($2\bar{1}\bar{1}0$). (Note: α_{Zn} is the O–Zn–O angle; α_O is the Zn–O–Zn angle; d_1 and d_2 are the surface Zn–O bond distances, as shown in figure 1(c).)

	Reconstruction				Relaxation							
Structure	α_{Zn} (deg)	α_O (deg)	d_1 (Å)	d_2 (Å)	Layer 1				Layer 2			
Clean ZnO	119.6	105.4	1.90	1.88	Zn 1	Zn 2	O 1	O 2	Zn 1	Zn 2	O 1	O 2
1_N	116	118	2.02	1.89	0.17	0.13	0.70	0.19	0.03	−0.06	−0.06	−0.02
2_N	72	92	2.83	1.96	0.21	0.30	0.21	0.16	0.11	−0.18	−0.06	−0.02
3_N	115	105	1.93	1.90	−0.14	0.05	0.10	0.07	0.01	0.02	0.00	−0.04

0.24 Å in magnitude, and an average displacement for this layer of 0.09 Å. Hence, relaxation of layers 1 and 2 caused by oxygen and nitrogen indicate that the adsorbates interact with both surface layers, however, the larger displacements observed in layer 1 indicate a stronger interaction with these atoms. The relaxations of the 3rd layer of surface atoms were <0.001 Å indicating, weaker interaction with the adsorbate.

In addition to the surface relaxations seen after adsorption of both atomic species, considerable surface reconstructions were also observed. Surface reconstructions were largest when the adsorbate atoms integrated themselves into the upper layer of the ZnO surface model distorting the structure of the clean surface (as seen in figures 2(a) and 3(a)). In these models the second layer atoms can be seen when inspecting the top view of the surface, whereas in the clean surface model they are aligned directly under the top layer of atoms. Milder surface reconstructions are apparent in the two-fold adsorption configurations where the second layer is almost completely obfuscated by the first layer, as seen in figures 2 and 3.

The geometric features characterizing surface reconstruction are listed in tables 3 and 4 and shown in figure 1(c), where α_{Zn} is the O–Zn–O angle; α_O is the Zn–O–Zn angle; and d_1 and d_2 are the surface Zn–O distances. The corresponding values for the clean relaxed surface are also presented. After adsorption, the d_1 length was found to increase for both oxygen and nitrogen systems, with the increase being in the range of 0.03–0.93 Å. Similarly, the d_2 length was found to increase in all systems, however, the bond length change was much smaller in magnitude, ranging from 0.01 to 0.08 Å. Adsorption also caused a distortion of the α_{Zn} and α_O angles, with the oxygen systems having a maximum α_{Zn} distortion of 19.6° and a maximum α_O distortion of 13.0°. The nitrogen systems had similar changes as reflected by their similar bonding arrangements, however, large changes of α_{Zn} of 47° and α_O of 13° were observed in structure 2_N. The changes in these distances as well as the measured angles after adsorption were found to specifically depend on which adsorbate–substrate bonds were formed. In structure 1_O the adsorbate does not bond to the surface Zn2 or O2 atom, hence, it is not surprising that the d_2 bond length barely changes. For structure 2_O, oxygen bonds to the surface Zn2 atom, resulting in an equal lengthening of d_1 and d_2 bonds. In structure 3_O, oxygen bonds to the surface Zn1 and Zn2 atoms, hence d_1 and d_2 both increase. As structure 1_N shows similar bonding to structure 1_O, the lengthening of the d_1 bond is similar. In structure 2_N, the large movements of the surface Zn2, O2 and O1 atoms result in large changes of d_1, α_O and α_{Zn}. For structure 3_N, where nitrogen bonds to only the surface Zn2 atom, both lengths change by similar amounts. Overall, the interaction of the adsorbates with the surface tends to weaken the strength of the Zn–O surface bonds directly involved in the bonding, resulting in a lengthening of the surface bond.

3.3. Workfunction changes

The workfunction changes of the adsorbate atoms (oxygen and nitrogen), as presented in tables 1 and 2, show that structures 2_O, 3_O and 3_N have a positive workfunction change, whereas structures 2_O, 1_N and 2_O have a negative workfunction change. If adsorbates induce a positive workfunction change, they withdraw electrons from the surface upon adsorption. Conversely, a negative workfunction change arises from a donation of charge from the adsorbate to the surface. Comparison of the six minimum structures reveals that a positive workfunction change occurs when oxygen or nitrogen interacts with surface zinc atoms only, whereas, a negative workfunction change arises when an oxygen or nitrogen interact with both surface zinc and oxygen atoms.

Osbourne *et al* [27] reported a drop in conductivity when sensors were exposed to a flux of atomic oxygen; this observation can be related to our calculated positive workfunction changes for structures 2_O and 3_O which indicated that oxygen withdraws charge from the ZnO surface. This removal of electrons from the surface, leads to increased resistance, i.e. a decrease in conductivity, supporting

Osbourne's observations. Surprisingly, the most stable structure 1_O has the opposite work function change. However, as we find more than one stable structure, it is possible that the experimentally measured work function change reflects a combination of all minima. As the magnitude of the work function change for structure 1_O is smaller than for structures 2_O and 3_O, the net change may still be positive, in agreement with experiment.

3.4. Vibrational frequencies

The symmetric stretch vibrational frequency of the adsorbed atomic species is presented in tables 1 and 2. For adsorbed oxygen, the stretching mode occurs over a smaller range of frequencies (362–595 cm^{-1}) than for adsorbed nitrogen (297–759 cm^{-1}). Furthermore, the magnitude of the symmetric vibrational frequency of the different structures is seen to depend upon the adsorption geometry, with the more highly coordinated adsorbates having larger symmetric stretches than the adsorbates that interact with a single surface atom. Hence, for structures 1_O and 1_N the calculated frequencies are the largest. Structures 3_O and 2_N, where oxygen and nitrogen interact with two surface atoms have the second largest frequencies. The lowest vibrational frequencies were calculated for the systems that involve adsorption onto a single zinc surface atom (structures 3_O and 2_N). In summary, it was found that as the degree of coordination increases, the peaks are further bathochromically (red) shifted. To the best of our knowledge there has been no Fourier transform infrared (FTIR), vibrational electron energy loss (VEELS) or reflection adsorption infrared spectroscopy (RAIRS) studies of the atomic species of oxygen and nitrogen adsorbing onto the ZnO($2\bar{1}\bar{1}0$) surface for comparison.

3.5. Charge density

Charge density difference plots and electron localization functions (ELF) of the minimum energy structures of O/ZnO($2\bar{1}\bar{1}0$) and N/ZnO($2\bar{1}\bar{1}0$) are presented in figures 4 and 5, respectively. The charge density difference slices are generated by subtracting the charge density of the clean surface and the isolated adsorbate atom (in their positions after O or N adsorption and relaxation) from that of the adsorbed surface structure. For each adsorbate, separate charge density and electron localization function plots were generated; these plots were aligned to cut through the adsorbate atom and its closest neighbouring surface atoms. High regions in ELF plots (indicated in red) can be interpreted as bonding and non-bonding electron pairs [37].

For structure 1_O, where the oxygen adsorbate (O_{ads}) interacts with both surface zinc (Zn_{surf}) and surface oxygen (O_{surf}) atoms, the electron density maps are taken along slice 1 (O_{ads}–O_{surf}) and slice 2 (O_{ads}–Zn_{surf}). Along the direction of the O_{ads}–O_{surf} bond in slice 1, there is a region of charge depletion followed by accumulation, then depletion. The symmetric distribution of charge accumulation/depletion between O_{ads} and O_{surf} suggests a covalent type of bonding. For the ELF plot, high regions of electron localization are found on the adsorbate and substrate oxygen atoms aligned perpendicular to the bond, representative of the p orbitals. In contrast, the charge density difference plot along slice 2 (O_{ads}–Zn_{surf}) mainly shows regions of charge accumulation and depletion located on the oxygen atom, with little change on the zinc atom. Such an uneven distribution suggests a degree of ionic character in this bond. This slice also cuts through the second layer zinc atom, showing a similar interaction with the O_{ads} as the top layer zinc atom, indicating most of the charge redistribution occurs between the adsorbate atom and the surface oxygen atom. Overall, the regions of charge accumulation, as well as depletion, located on the adsorbate atom may result in the small work function change observed for this structure.

The charge density difference plots and ELF of structure 2_O shows a smaller redistribution of charge, consistent with the smaller binding energy value of this structure. Along the O_{ads}–Zn_{sub} bond (slice 1) there is a region of charge accumulation close to the oxygen atom, while there is a region of depletion around the Zn atom, indicating a bond of ionic nature. Furthermore, there is a large region of charge depletion around the oxygen atom in the direction away from the bond. In the ELF plot, the region of high localization occurs on the adsorbate oxygen atom, similar to in the bulk, indicating that the bonding is similar and mainly ionic in nature.

The charge density difference and ELF slices of structure 3_O, shown along slice 1 (Zn_{sub}–O_{ads}–Zn_{sub}), indicate that the oxygen adsorbate atom has formed an ionic-type bond to both surface zinc atoms as going along the two bonds, there is a region of charge depletion close to either zinc atom and a region of accumulation close to the adsorbate oxygen atom. As one zinc atom is 0.13 Å closer to the adsorbate than the other, the charge depletion is larger, indicating a stronger interaction between the closer atoms. The ELF plot confirms the mainly ionic character of the bond, with localized electron pairs residing on the oxygen adsorbate atom. The charge density difference plots of structures 2_O and 3_O indicate an overall withdrawal of charge from the surface, in line with the calculated positive workfunction changes. It is noteworthy that the sign of the workfunction change is affected by the surface atoms that the adsorbate interacts with. Positive workfunction changes were calculated for both adsorbed oxygen and nitrogen if the adsorbate bonded with zinc atoms. Similarly, negative workfunction changes were calculated when the adsorbate interacted with both surface oxygen and zinc atoms. Interactions between the adsorbate and the surface zinc atoms resulted in ionic-type bonding, whereas, interactions with oxygen atoms were more likely to results in the formation of covalent-type bonding. The small negative workfunction change of structure 1_O is most likely due to donation of charge to the surface in an attempt to stabilize the covalent-type bond observed in slice 1.

For structure 1_N, the charge density difference plots again show large regions of charge accumulation and depletion. Going along slice 1 (N_{ads}–O_{sub}), there is a region of depletion followed by accumulation and then depletion, similar to what was observed in slice 1 of structure 1_O. Again, there are regions of charge accumulation perpendicular to the bond direction, located on the oxygen and nitrogen atoms, resembling p orbital

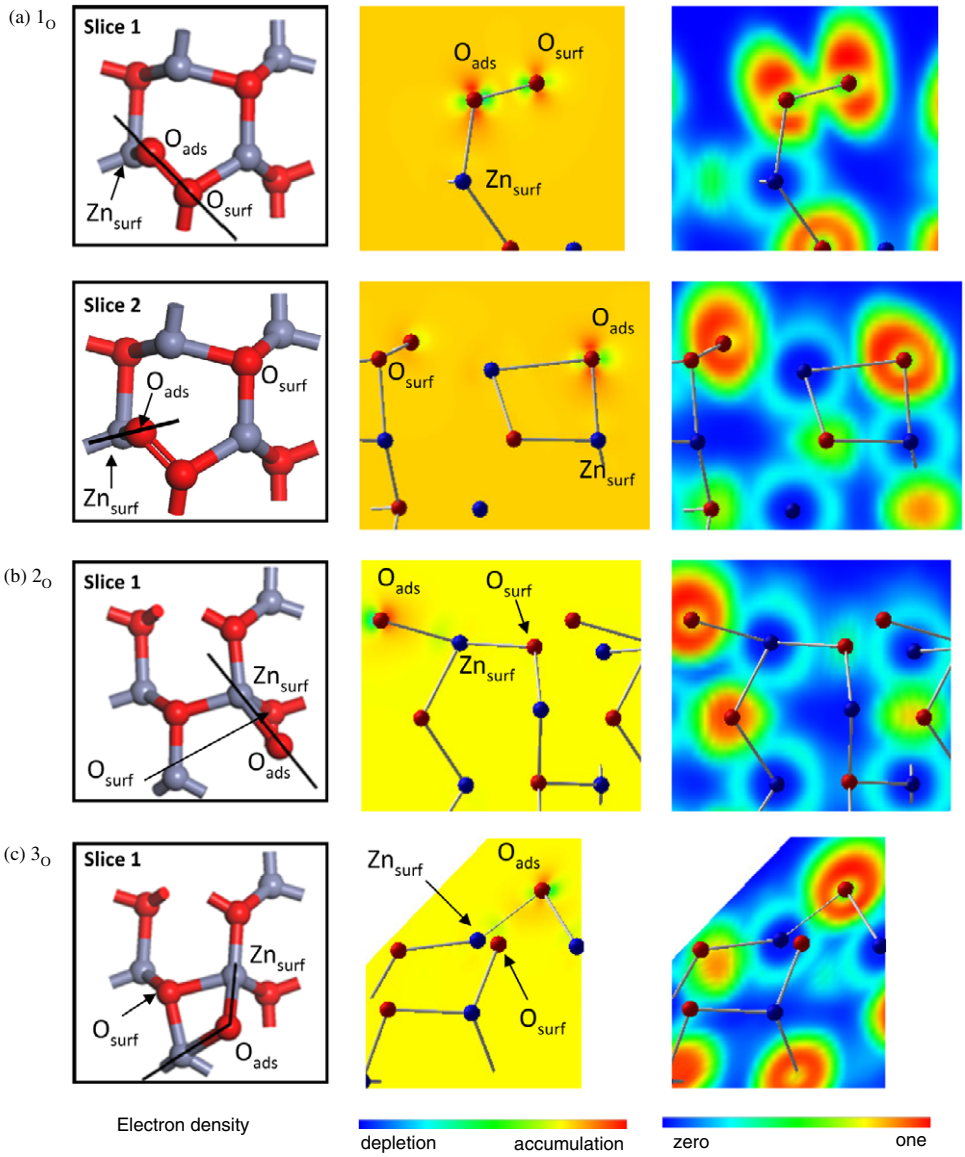

Figure 4. Charge density difference plots (middle) and ELF plots (right) of the O/ZnO($2\bar{1}\bar{1}0$) structures, (oxygen atoms denoted in red and zinc atoms in blue). The slices are taken along the shortest adsorbate–substrate distances, as indicated on the top view of the structures (left).

lobes. Such changes again indicate a high degree of covalency in the bonding. In the ELF plot, there is again a large region of localization on both the oxygen atom and adsorbate nitrogen atom, just as in structure 1_O. Slice 2 (N_{ads}–Zn_{sub}) highlights a distinct accumulation of charge on the nitrogen adsorbate atom suggesting an ionic interaction with the surface zinc atom. This is accompanied by a small depletion of charge located around the surface zinc atom. This is not observed in slice 2 of the 1_O system, as the geometry of the 1_N system is more highly strained than that of the 1_O system. Comparing structures 1_O and 1_N in figures 2 and 3, respectively, it can be clearly seen that the bonds formed in the top layer of structure 1_O are longer than those in structure 1_N. The ELF plot of structure 1_N (N_{ads}–Zn_{surf}) exemplifies this withdrawal of charge from surrounding atoms, visible as distortions in the lobes of the orbitals on the nitrogen adsorbate atom. The close proximity of the nitrogen adsorbate atom to the surface has an interesting effect on the calculated workfunction change. For both structures 1_N and 2_N, the charge density difference and ELF plots show that the nitrogen atom is close enough to neighbouring surface atoms to affect the electron density of atoms in the second layer. This proximity is anticipated to cause the nitrogen atom to donate electronic charge to its immediate surroundings, which results in a negative workfunction change.

The charge density difference plot of structure 2_N, along slice 1 (N_{ads}–O_{sub}) indicates covalent bonding between these atoms. The ELF plot shows a significant flaring of the nitrogen atom p orbitals in the z-direction away from the surface. Slice 2 (N_{ads}–Zn_{surf}) shows a somewhat unusual pattern of electron density between the nitrogen and zinc atom, with a region of charge depletion near the zinc atom and a region of accumulation near the nitrogen atom. This region of accumulation lies along the bond as well as perpendicular to the surface. This unusual density profile creates an ELF plot

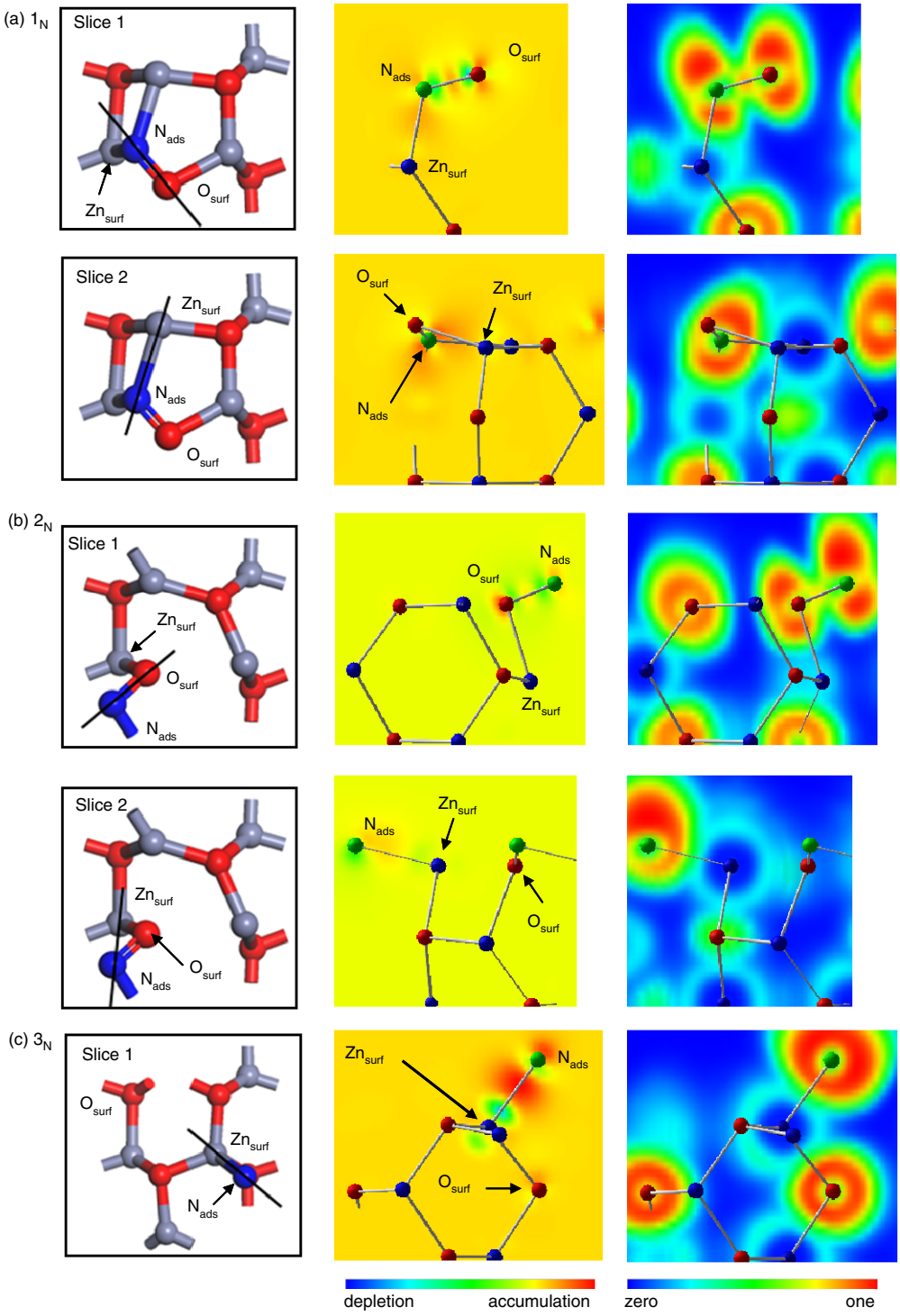

Figure 5. Charge density difference plots (middle) and ELF plots (right) of the N/ZnO($2\bar{1}\bar{1}0$) structures, (oxygen atoms denoted in red, nitrogen atoms in green, and zinc atoms in blue). The slices are taken along the shortest adsorbate–substrate distances, as indicated on the top view of the structures (left).

that has a region of paired electrons on the nitrogen adsorbate atom which lies along the bond as well as located away from the surface.

The charge density difference and ELF plots of the least stable structure 3_N still contain considerable charge differences despite the small binding energy value of −0.12 eV. Moving along the bond from the zinc atom to the nitrogen adsorbate atom, there is a large depletion of charge, followed by an accumulation near the nitrogen atom. There is also a small region of charge depletion near the nitrogen atom which indicates an ionic bond with some covalent character. It is noteworthy that the accumulation of charge on the nitrogen atom has also affected the oxygen atom directly underneath it. The small accumulation of charge on a second layer atom

was not observed in the other structures. The accumulation of electron density on the nitrogen adsorbate is also responsible for the positive workfunction change of 0.07 eV.

4. Conclusion

The interactions between the ZnO surface and the atomic oxygen and nitrogen adsorbates are for the most part strong, indicating chemisorption. The most stable oxygen adsorbate had a binding energy of −2.47 eV, while the most stable nitrogen adsorbate had a binding energy of −1.42 eV, indicating that oxygen binds more strongly on the ZnO($2\bar{1}\bar{1}0$) surface. In these two structures the adsorbate bonded to two or three surface atoms. Two additional local minimum structures were found for oxygen as well as for nitrogen, where the adsorbate atom bonded to only one or two surface atoms, resulting in less stable structures. Surface relaxation after adsorption was found to be largest in the top two surface layers, and negligible in subsequent layers, indicating the interaction between the adsorbate and surface was primarily confined to the surface region. Surface reconstructions were also observed, being prominent for the most stable minima of both adsorbates, but minor in the less stable structures. Both ionic-and covalent-type bonds were observed between the adsorbate and the surface. When the oxygen or nitrogen bonded to a surface oxygen atom, a bond of mainly covalent nature was formed. In contrast, when the adsorbates bonded to a surface Zn atom the bond was mainly ionic in nature with some covalent character. Workfunction calculations showed positive changes for adsorption in less highly coordinated sites and negative changes for more highly coordinated atomic species. The positive workfunction changes of adsorbed oxygen may be correlated with the experimentally observed decreases in conductivity of ZnO conductometric sensor technologies. Conversely, it is hypothesized that the large negative workfunction change calculated for Structures 1_N and 2_N would cause the ZnO sensor to decrease in resistance, resulting in an increase in conductivity upon exposure to nitrogen, effectively functioning in the opposite mode of operation when compared with exposure to oxygen. The ZnO($2\bar{1}\bar{1}0$) surface may prove to be useful in the development of an atomic nitrogen sensor.

Acknowledgments

This research was supported under the Australian Research Council's *Discovery Projects* funding scheme (project number DP0666883). The Australian Partnership for Advanced Computing (APAC) for providing computational facilities.

References

[1] Song J H, Zhou J and Wang Z L 2006 Piezoelectric and semiconducting coupled power generating process of a single ZnO belt/wire. A technology for harvesting electricity from the environment *Nano Lett.* **6** 1656–62

[2] Baxter J B and Aydil E S 2005 Nanowire-based dye-sensitized solar cells *Appl. Phys. Lett.* **86** 053114

[3] Liu Q, Zhang W-M, Cui Z-M, Zhang B, Wan L-J and Song W-G 2007 Aqueous route for mesoporous metal oxides using inorganic metal source and their applications *Micropor. Mesopor. Mater.* **100** 233–40

[4] Koshizaki N and Oyama T 2000 Sensing characteristics of ZnO-based NOx sensor *Sensors Actuators* B **66** 119–21

[5] Soci C *et al* 2007 ZnO nanowire UV photodetectors with high internal gain *Nano Lett.* **7** 1003–9

[6] Ng H T, Han J, Yamada T, Nguyen P, Chen Y P and Meyyappan M 2004 Single crystal nanowire vertical surround-gate field-effect transistor *Nano Lett.* **4** 1247–52

[7] Wang X D, Song J H and Wang Z L 2006 Single-crystal nanocastles of ZnO *Chem. Phys. Lett.* **424** 86–90

[8] Wang Z L 2004 Nanostructures of zinc oxide *Mater. Today* **7** 26–33

[9] Wang Z L 2006 Novel zinc oxide nanostructures discovery by electron microscopy *J. Phys.: Conf. Ser.* **26** 1–6

[10] Comini E 2006 Metal oxide nano-crystals for gas sensing *Anal. Chim. Acta.* **568** 28–40

[11] Sadek A Z, Wlodarski W, Li Y X, Yu W, Li X, Yu X and Kalantar-zadeh K 2007 A ZnO nanorod based layered ZnO/64° YX $LiNbO_3$ SAW hydrogen gas sensor *Thin Solid Films* **515** 8705–8

[12] Heo Y W *et al* 2004 ZnO nanowire growth and devices *Mater. Sci. Eng.* R **47** 1–47

[13] Lupan O, Chai G and Chow L 2007 Fabrication of ZnO nanorod-based hydrogen gas nanosensor *Microelectron. J.* **38** 1211–6

[14] Casarin M, Maccato C and Vittadini A 1999 A theoretical investigation of the relaxation effects induced on the ZnO(1010) surface by the chemisorption of H_2 and CO *Appl. Surf. Sci.* **142** 192–5

[15] Cooke D J, Marmier A and Parker S C 2006 Surface structure of (1010) and (1120) surfaces of ZnO with density functional theory and atomistic simulation *J. Phys. Chem.* B **110** 7985–91

[16] Kunat M, Meyer B, Traeger F and Woll C 2006 Structure and dynamics of CO overlayers on a hydroxylated metal oxide: the polar ZnO(0001) surface *Phys. Chem. Chem. Phys.* **8** 1499–504

[17] Martins J B L, Moliner V, Andres J, Longo E and Taft C A 1995 A theoretical study of water adsorption on ($10\bar{1}0$) and (0001) ZnO surfaces: molecular cluster, basis set and effective core potential dependence *J. Mol. Struct. Theochem.* **330** 347–51

[18] Meyer B 2004 First-principles study of the polar O-terminated ZnO surface in thermodynamic equilibrium with oxygen and hydrogen *Phys. Rev.* B **69** 045416

[19] Wander A and Harrison N M 2000 An *ab initio* study of ZnO(1010) *Surf. Sci.* **457** L342–6

[20] Wander A and Harrison N M 2000 An *ab initio* study of ZnO(1120) *Surf. Sci.* **468** L851–5

[21] Zapol P, Jaffe J B and Hess A C 1999 *Ab initio* study of hydrogen adsorption on the ZnO surface *Surf. Sci.* **422** 1–7

[22] Wang C C, Zhou G, Li J, Yan B H and Duan W H 2008 Hydrogen-induced metallization of zinc oxide ($2\bar{1}\bar{1}0$) surface and nanowires: the effect of curvature *Phys. Rev.* B **77** 245303

[23] Nyberg M, Nygren M A, Pettersson L G M, Gay D H and Rohl A L 1996 Hydrogen dissociation on reconstructed ZnO surfaces *J. Phys. Chem.* **100** 9054–63

[24] Yan Y, Al-Jassim M M and Wei S-H 2005 Oxygen-vacancy mediated adsorption and reactions of molecular oxygen on the ZnO($10\bar{1}0$) surface *Phys. Rev.* B **72** 161307

[25] WHO 2005 *Air Qualities Guidlines Global Update 2005*

[26] Francesco Forastiere A P, Frank J K and Stephen T H 2005 *Air Qualities Guidlines Global Update 2005* World Health Organisation (WHO)

[27] Osborne J J, Roberts G T, Chambers A R and Gabriel S B 2000 Thin-film semiconductor sensors for hyperthermal oxygen atoms *Sensors Actuators* B **63** 55–62
[28] Kresse G and Furthmuller J 1996 Efficiency of *ab initio* total energy calculations for metals and semiconductors using a plane-wave basis set *Comput. Mater. Sci.* **6** 15–50
[29] Kresse G and Furthmüller J 1996 Efficient iterative schemes for *ab initio* total-energy calculations using a plane-wave basis set *Phys. Rev.* B **54** 11169
[30] Kresse G and Hafner J 1993 *Ab initio* molecular dynamics for open-shell transition metals *Phys. Rev.* B **48** 13115
[31] Kohn W and Sham L J 1965 Self-consistent equations including exchange and correlation effects *Phys. Rev.* **140** A1133
[32] Perdew J P and Wang Y 1992 Accurate and simple analytic representation of the electron–gas correlation energy *Phys. Rev.* B **45** 13244
[33] Vanderbilt D 1990 Soft self-consistent pseudopotentials in a generalized eigenvalue formalism *Phys. Rev.* B **41** 7892
[34] Monkhorst H J and Pack J D 1976 Special points for Brillouin-zone integrations *Phys. Rev.* B **13** 5188
[35] Spencer M J S, Yarovsky I, Wlodarski W and Kalantar-zadeh K 2007 Density functional theory study of ZnO nanostructures for NO and NO_2 sensing *Proc. of Transducers and Eurosensors '07 (Lyon, June 2007)* pp 987–90
[36] Spencer M J S, Snook I K and Yarovsky I 2006 Effect of S arrangement on Fe(110) properties at 1/3 monolayer coverage: a DFT study *J. Phys. Chem.* B **110** 956–62
[37] Terriberry T B, Cox D F and Bowman D A 2002 A tool for the interactive 3D visualization of electronic structure in molecules and solids *Comput. Chem.* **26** 313–9